

High-field magnetoresistance of the Bechgaard salt $(\text{TMTSF})_2\text{NO}_3$: Quantum oscillations in the spin-density-wave state and phase transitions

Alain Audouard, Frédéric Goze, Jean-Pierre Ulmet, Luc Brossard, and Salomon Askenazy
*Service National des Champs Magnétiques Pulsés (CNRS-UMS 819), Laboratoire de Physique des Solides (CNRS URA 074),
 Complexe Scientifique de Rangueil, 31077 Toulouse, France*

Jean-Marc Fabre

*Laboratoire de Chimie Organique Structurale, Université des Sciences et Techniques du Languedoc, place Eugène Bataillon,
 34095 Montpellier Cedex 5, France*

(Received 4 March 1994; revised manuscript received 27 May 1994)

The transverse magnetoresistance of the Bechgaard salt $(\text{TMTSF})_2\text{NO}_3$ has been measured up to 37 T at ambient pressure in the temperature range from 2 to 77 K. When the magnetic field is parallel to the lowest conductivity direction c^* and for temperatures higher than ~ 12 K, the data can be accounted for by a power law, the exponent of which decreases as the anion ordering takes place. At lower temperatures, the magnetic field increases the spin-density-wave (SDW) transition temperature, in overall agreement with theoretical predictions for the imperfect-nesting case. Two oscillation series, both linked to the SDW state, have been observed in the 2–10 K range. Their temperature-independent frequencies, measured from 2 to 8 K, are at (63 ± 2) and (248 ± 5) T, respectively. These oscillations have been studied (at 4.2 K) as a function of the field direction. They were found to deviate from the two-dimensional model since, in particular, their behavior differs according to whether the field is tilted on one side of the c^* direction or on the other. The oscillation data are discussed on the basis of recent calculations of Yakovenko.

I. INTRODUCTION

Bechgaard salts, $(\text{TMTSF})_2X$, where TMTSF stands for the tetramethyltetraselenafulvalene donor molecule and X is an anion such as PF_6 , ClO_4 , NO_3 , ReO_4 , etc., are well-known quasi-one-dimensional (quasi-1D) organic conductors. Depending on applied pressure and/or thermal history, their ground state can be either superconducting (PF_6 salt under pressure¹ or slowly cooled ClO_4 salt²), metallic [NO_3 salt above 8 kbar (Ref. 3)], or semiconducting, due to the condensation of a spin-density-wave (SDW) instability [ambient-pressure NO_3 (Ref. 4) and PF_6 salts^{5,6} or quenched ClO_4 salt^{7,8}]. In addition, compounds with noncentrosymmetric anions (NO_3 and slowly cooled ClO_4 salts⁹) may undergo anion ordering (AO). Starting from a superconducting (SC) ground state, a magnetic field (B) applied along the lowest-conductivity c^* axis restores first a semimetallic state. The so-called field-induced spin-density-wave (FISDW) cascade is further induced,^{10–14} giving rise to a quantum Hall effect^{15–17} and to magnetoresistance (MR) bumps, periodic in $1/B$, which are the signature of transitions between the successive FISDW phases. In PF_6 (Ref. 10) and ClO_4 (Ref. 14) salts, the measured frequency is at 76 and 35 T, respectively, while in the ReO_4 salt¹⁷ two frequencies at 33 and 111 T have been, respectively, evidenced below and above 16 T. Furthermore, if the field is tilted in the lowest-conductivity plane, a commensurability resonance (CR) phenomenon occurs, as predicted,¹⁸ at special field directions called magic angles.

The FISDW phenomenon is now rather well under-

stood and currently interpreted on the basis of a field-induced quantization of the nesting vector.¹⁹ However, MR data also exhibit, roughly in the temperature and pressure range where FISDW's occur, so-called fast oscillations (FO's), which remain a puzzling problem. As a matter of fact, these oscillations have been observed in the three salts with ClO_4 ,^{14,20} PF_6 ,²¹ and ReO_4 (Refs. 17 and 22) anions, although the topology of their Fermi surface (FS) does not allow for the Shubnikov–de Haas (SdH) effect. Indeed, only open orbits remain in the metallic ground state of ClO_4 and ReO_4 salts, and very small closed ones, if any, set up in the SDW state of the PF_6 salt as a result of the quasiperfect SDW nesting. The frequencies (B_F) of these FO's, which are temperature independent, are in the range 230–330 T in the above three salts, i.e., much larger than the frequencies linked to the FISDW transitions. It can be noted that, for the perchlorate compound, two out-of-phase FO series with the same frequency have been observed in the FISDW state.^{14,20} Both the magnetic field and temperature dependences of the amplitude of FO's as well as their existence in both metallic and SDW phases (without any phase or frequency discontinuity at the FISDW transitions) have not been understood yet.

Among the Bechgaard salts, $(\text{TMTSF})_2\text{NO}_3$ is a good candidate to bring new pieces to the puzzle since it exhibits several features of peculiar interest. Indeed, contrary to AO in most other salts, the $(\frac{1}{2}, 0, 0)$ AO wave vector⁹ should lead to closed orbits. The SDW order parameter at zero temperature is only about 8 K,²³ and the temperature dependence of the resistivity in the SDW state sug-

gest imperfect nesting. In addition, although a metallic state is stabilized under pressure, no SC ground state has been observed whatever the pressure up to 24 kbar.²⁴ According to Yakovenko,²⁵ the FISDW cascade should be closely connected to the presence of a SC ground state. This is the reason why attention has recently been focused on the behavior of $(\text{TMTSF})_2\text{NO}_3$ under a magnetic field. In agreement with the predictions of Ref. 25, no FISDW rising from the metallic phase has been observed up to 30 T.³ On the other hand, most of the experiments reported in the SDW state deal with a low magnetic field.^{3,26,27} In a previous paper,²⁸ preliminary high-magnetic-field transverse MR data were reported in the SDW ground state with \mathbf{B} parallel to c^* : Two series of quantum oscillations were observed in the temperature range 2–10 K which have been interpreted in the framework of field-induced tunneling which occurs through FS breakdowns related to SDW gap openings. The present paper reports on (i) AO and SDW phase transitions under high magnetic field and (ii) angular dependence of the oscillatory behavior of the MR. To that purpose, the MR was measured up to 37 T in the range 2–77 K, with $\mathbf{B} \parallel c^*$ [point (i)] and the angular behavior of the MR oscillations [\mathbf{B} in the (b', c^*) plane] was explored at liquid-helium temperature where the oscillation amplitude is the largest [point (ii)]. It is worthwhile to note that Biskup *et al.*²⁹ also report on the MR behavior of $(\text{TMTSF})_2\text{NO}_3$. Their data, which deal with low-field measurements (up to 12 T) in the temperature range from 1.2 to 7 K, are in agreement with ours.

II. EXPERIMENTAL DETAILS

Three single crystals were studied. Samples were classically mounted in the four-point geometry with gold wires (17.5 μm in diameter) stuck with gold paste on preevaporated gold contacts. The amplitude of 50 kHz ac current, flowing along the best conduction direction (a axis), was low enough ($\sim 15 \mu\text{A}$) to avoid Joule heating and possible non-Ohmic effects. The signal across potential contacts was filtered to remove field-induced voltages and amplified by a bandpass amplifier. It was then demodulated and driven to a data-acquisition unit. To avoid cracks, the samples were slowly cooled ($\sim 0.1 \text{ K min}^{-1}$) from 300 down to 2 K so that the standard temperature dependence of the resistance was obtained;⁴ namely, a metallic behavior was observed down to 12 K, followed by a steep resistance increase due to the condensation of the SDW phase. The temperatures at which SDW and AO transitions take place were conventionally estimated²³ from the extrema of $d[\ln(R)]/d(1/T)$. This parameter exhibits a minimum at $T_{\text{AO}} = 41 \text{ K}$ and a maximum at $T_{\text{SDW}} = 9.4 \text{ K}$, both in good agreement with data of the literature.^{9,23}

Magnetoresistance measurements were carried out in pulsed magnetic fields up to 37 T during the decay period (1.2 s) of the magnetic field, in the transverse configuration ($\mathbf{B} \perp a$). A sample holder rotating about an axis perpendicular to \mathbf{B} allowed a 360° variation of the (\mathbf{B}, c^*) angle in the lowest conductivity (b', c^*) plane, where b' is the projection of the b axis perpendicularly to

a . Crystal orientation was achieved by assigning the b' direction to the orientation where the magnetoresistance was the lowest, as usual, for TMTSF salts.²⁶

III. RESULTS AND DISCUSSION

The resistivity ratio $R(300 \text{ K})/R(12 \text{ K})$ was 25, 80, and 93 for sample 1, 2, and 3, respectively. All three studied crystals exhibited the same behavior. Figure 1 collects transverse MR ($\Delta R/R_0$) data recorded at different temperatures in the range 2–20 K for \mathbf{B} parallel to the c^* axis. For temperatures higher than 10 K, i.e., above T_{SDW} , a monotonous magnetic field dependence of the resistance is observed. At lower temperatures, quantum oscillations of the MR are also evidenced as previously reported.^{3,28} This section is therefore divided into two parts. In Sec. III A, semiclassical effects are only considered in relation to AO and SDW phase transitions, for a magnetic field parallel to the c^* axis, while Sec. III B deals with the angular dependence of the transverse magnetoresistance oscillations measured at 4.2 K.

A. Phase transitions

In the temperature range from 77 down to 12 K, i.e., above the onset of the SDW condensation, the transverse MR ($\mathbf{B} \parallel c^*$) can be accounted for by a power law ($\Delta R/R_0 \approx B^n$) in the whole magnetic field range covered by the experiments (see Fig. 2). At temperatures higher than 50 K, the measured power-law exponent is $n = 2.8$. A close value ($n \sim 3$) has also been observed in the quasi-1D metallic state of the organic compound $(\text{TSeT})_2\text{Cl}$.³⁰ As the temperature decreases, a curvature variation is evidenced in the data of Fig. 2, leading to a decrease of n down to 1.8 in the 20–12 K range (Fig. 3). Such a variation of the power-law exponent (although from 2 down to ~ 1) has also been observed in the relaxed ClO_4 salt around 24 K.³¹ As evidenced in Fig. 3, this behavior is linked to AO since an inflexion point takes place at T_{AO} . It is worthwhile to note that the temperature dependence of the power-law exponent is in surprisingly good agree-

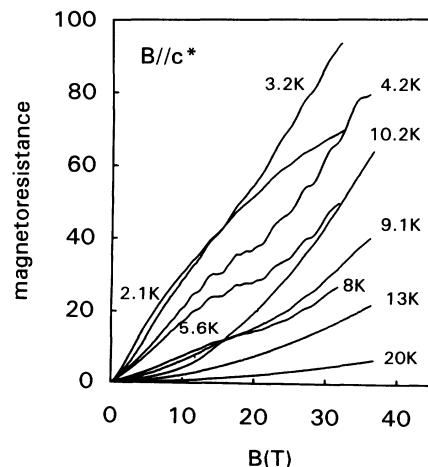


FIG. 1. Transverse magnetoresistance ($\Delta R/R_0$) of sample 3 recorded at different temperatures for \mathbf{B} parallel to c^* .

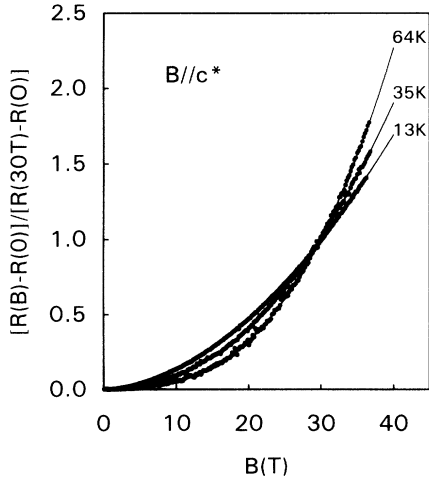


FIG. 2. Transverse magnetoresistance of sample 3 recorded in the temperature region where the anion ordering occurs. The data are normalized at 30 T in order to evidence the curvature change. Circles are experimental data and lines are best fits to a power law.

ment with that of the order parameter as determined by x-ray diffuse scattering experiments.⁹

At lower temperature, i.e., as soon as the SDW phase starts to condense, the above power law is no more valid. The evolution of the semiclassical part of the MR, as the temperature varies, becomes then rather complicated since, e.g., the MR is higher at 10.2 K than at 8 K (see Fig. 1). This peculiar behavior is even more clearly evidenced in Fig. 4, which shows the temperature dependence of the MR for different \mathbf{B} values: While, at $\mathbf{B} < 15$ T, the MR decreases monotonously as the temperature increases, a maximum appears at about 10 K for $\mathbf{B} \geq 15$ T and another maximum can further be seen at about 3 K as soon as \mathbf{B} reaches 20 T.

The maximum observed at 10 K in Fig. 4 is likely connected to the SDW transition. Such a large effect may be accounted for not only by a relaxation time decrease due to short-range spin fluctuations³² and/or by some enhancement of the thermal fluctuations of the order parameter,³³ but also by some field-induced increase in T_{SDW} . Indeed, as demonstrated in Fig. 5 where

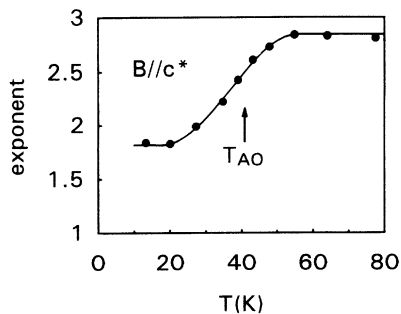


FIG. 3. Temperature dependence of the power-law exponent (n) deduced from best fits to magnetoresistance data (some examples are given in Fig. 2).

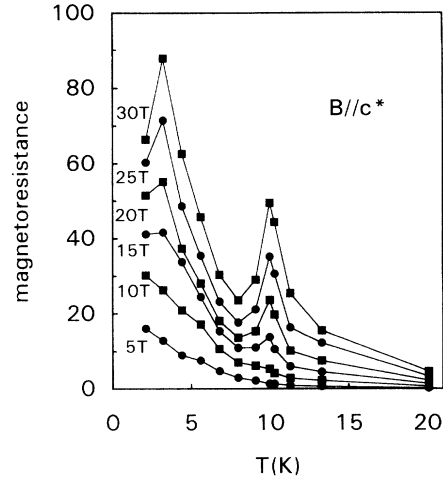


FIG. 4. Temperature dependence of the semiclassical part of the transverse magnetoresistance of sample 3 measured for different magnetic fields.

$d[\ln(R)]/d(1/T)$ is plotted as a function of temperature for different magnetic field values, T_{SDW} increases as the magnetic field increases (see Fig. 6). This variation is also evidenced by the large field-induced increase of the resistance which can be seen in MR data measured in the temperature range close to 10 K (see the curve recorded at 10.2 K in Fig. 1). The T_{SDW} variation is substantial (14% at 30 T), in agreement with Montambaux³⁴ who has calculated the field dependence of T_{SDW} with a nesting departure. As a matter of fact, the low-temperature dependence of the conductivity is in poor agreement with a thermally activated behavior;²³ the SDW nesting is thus thought to be imperfect.²⁶ Mean-field calculations³⁴ predict a quadratic field dependence of T_{SDW} in the limit of low magnetic field and for temperatures higher than the transfer energy t_c :

$$T_{\text{SDW}}(\mathbf{B}) = T_{\text{SDW}}(0) + f \left[\frac{t'_b}{t_b^{**}} \right] \frac{\omega_c^2}{t_b^{**}}, \quad (1)$$

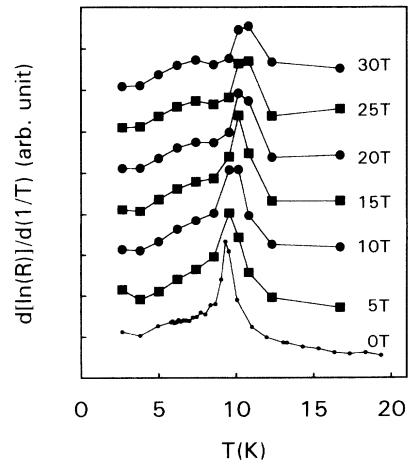


FIG. 5. Temperature dependence of $d[\ln(R)]/d(1/T)$ for different magnetic fields (sample 3).

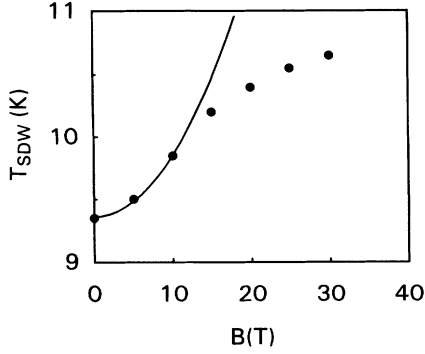


FIG. 6. Magnetic field dependence of T_{SDW} . Circles are deduced from Fig. 5, and the solid line is a fit of Eq. (1) to the low-field part of the data.

where f is a universal function which increases as the nesting becomes more and more imperfect, t'_b is the characteristic energy of the deviation from perfect nesting, and t'_b^* is its critical value above which no SDW transition can occur. At a magnetic field such that $\hbar\omega_c > t'_b$, where ω_c is the cyclotron pulsation, Eq. (1) is no longer valid and the magnetic field dependence of T_{SDW} should saturate. The data in Fig. 6 are in full agreement with the above reported behavior. First, the quadratic dependence predicted by Eq. (1) is fulfilled up to ~ 10 T: The solid line in Fig. 6 is a fit to the data in the low-field range which yields $f(t'_b/t'_b^*)/t'_b^* = 0.005 \text{ K}^{-1}$. This value is roughly a factor of 5 lower than for the PF_6 salt under a pressure of 6 kbar, i.e., close to the critical pressure p_c at which $t'_b = t'_b^*$.³⁵ The observed agreement is quite surprising, since not only the actual dispersion relation, but also the FS's of the NO_3 salt are more complex than the one used in Ref. 34. Despite this complexity, it is worthwhile to note that a simple model essentially based on a single parameter t'_b is able to nicely reproduce experimental data. Hence the above analysis ensures the assumption²⁶ that the SDW phase of the NO_3 salt illustrates an intermediate case between perfect nesting (e.g., PF_6 salt at ambient pressure) and strongly imperfect nesting (e.g., PF_6 salt at a pressure just below p_c).

As the temperature further decreases, the shape of the MR curves changes again. A semilogarithmic plot exhibits an inflexion point at low magnetic field in the temperature range up to ~ 6 K (Fig. 7). According to Ref. 36, such a behavior could be explained by magnetic breakthrough. In that framework, the magnetic field B_{in} at which the inflexion point occurs is linked to the magnetic breakthrough field given by $B_0 = \Delta^2 m_c / e \hbar E_F$,³⁷ where E_F is the pertinent kinetic energy, m_c is the cyclotron mass, and Δ is the energy barrier between two orbits. In the present case, Δ is the temperature-dependent SDW gap. As demonstrated in Fig. 7, B_{in} increases as the temperature decreases. This is in qualitative agreement with the continuous SDW gap opening, which should occur down to about $T_{\text{SDW}}/4$, i.e., ~ 2.5 K.

Finally, high-field MR is lower at 2.1 K than at 3.2 K (see Figs. 1 and 4). This is reminiscent of the ambient-

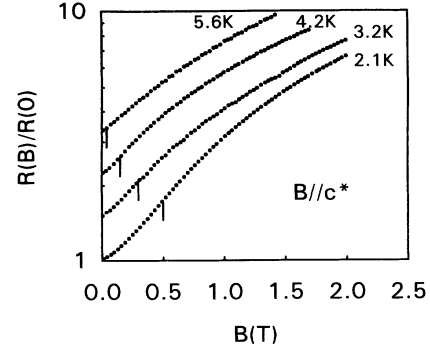


FIG. 7. Semilogarithmic plot of the magnetoresistance of sample 3 in the temperature range 2.1–5.6 K. Marks indicate inflexion points B_{in} (see text). The curves are shifted by a factor 1.5 from each other for the sake of clarity.

pressure behavior of the PF_6 salt, which displays a sharp decrease of the MR as the temperature decreases from 5 to 3.8 K.³⁸ Such a feature could be the precursor effect of a glass transition which has been shown to take place at 2–3 K in the PF_6 salt,³⁹ in agreement with a previous suggestion of a wide distribution of metastable pinned SDW configurations.⁴⁰

B. Magnetoresistance oscillations

Low-field MR experiments performed at ambient pressure by Kang *et al.*³ have revealed quantum oscillations, with frequency $B_F = (75 \pm 10)$ T. Two series were previously evidenced in the transverse MR, in the range 2–10 K, for $B \parallel c^*$.²⁸ Their respective frequencies are $B_{FL} = (63 \pm 2)$ T, which is in agreement with Ref. 29 and not too far from the data of Ref. 3, and $B_{FH} = (248 \pm 5)$ T. The data in Fig. 1 yield $B_{FL} = (63.5 \pm 1)$ T and $B_{FH} = (246 \pm 3)$ T, in very good agreement with our previous values. The low-frequency series (L) appears at low magnetic field, while the high-frequency one (H) only appears beyond ~ 16 T. It can be remarked that B_{FH} is close to the FO frequency in other Bechgaard salts,^{16,17,20–22} while B_{FL} is not far from the frequency of the MR anomalies, attributed to transitions between the different FISDW phases in PF_6 (Ref. 10) and ClO_4 (Ref. 14) salts. However, contrary to these magnetoresistance anomalies, the oscillations observed in the NO_3 salt have a clear sinusoidal shape. It has been pointed out²⁸ that both oscillation series are not linked to AO, but merely to the SDW phase, owing to the fact that, in the metallic state stabilized at 0.5 K above 8 kbars,³ no MR oscillation can be seen. While high-frequency series can likely be identified as FO's, usually observed in Bechgaard salts, the low-frequency one has no counterpart in other salts (in particular, it is not linked to any cascade of FISDW transitions). Thus it should not seem unrealistic to assume (i) that the low-frequency series is linked to residual carrier pockets due to the SDW imperfect nesting and thus (ii) that the SdH model could be valid here. Oppositely, we have verified that, at a given temperature, the

magnetic field dependence of the L -series oscillation amplitude is not in agreement with the predictions of the SdH model. In addition, in the whole temperature range where B_{FL} and B_{FH} can be measured (here from 2 to 8 K, i.e., up to $0.85 T_{SDW}$), they are both temperature independent, which also rules out the SdH model. Indeed, in this framework, $B_{FL(H)}$ should be proportional to the area of the carrier pockets left by the SDW transition. Thus $B_{FL(H)}$ should decrease as the order parameter increases, i.e., as the temperature decreases, which is not the case.

The anisotropy of the oscillatory part of the MR was studied at 4.2 K, i.e., in the temperature range where the oscillation amplitude of both series is the largest. The data measured at different (\mathbf{B}, c^*) tilt angles is plotted in Fig. 8 as a function of $1/[\mathbf{B} \cos(\mathbf{B}, c^*)]$. The sign of the (\mathbf{B}, c^*) angle is taken as arbitrary. The periodicity of the oscillations has been systematically checked. Indeed, the data can be plotted according to the Onsager relation

$$1/B_n = (n + \gamma)/B_{FL(H)}, \quad (2)$$

where B_n is the field value at a given oscillation maximum and n is chosen such that the phase factor γ lies between 0 and 1 for \mathbf{B} parallel to the c^* axis. A good agreement with Eq. (2) is observed as well for the L as for the H series except, in the latter case, for few tilt angles in the \mathbf{B} range where the L and H series are strongly mixed. As can be seen in Fig. 8, the data are not in very good agreement with a 2D behavior since $B_n \cos(\mathbf{B}, c^*)$ progressively shifts toward low-field values as (\mathbf{B}, c^*) increases. The angular dependence of B_{FL} and B_{FH} , is, respectively, displayed in Figs. 9(a) and 9(b). The cosine

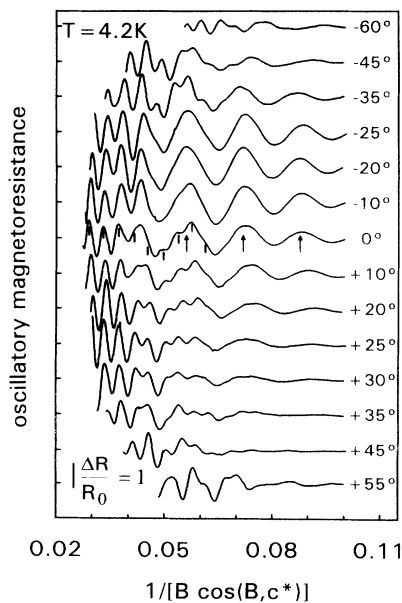


FIG. 8. Oscillatory part of the transverse magnetoresistance of sample 2 at 4.2 K for different (\mathbf{B}, c^*) tilt angles indicated on each curve. The data are plotted as a function of $1/[\mathbf{B} \cos(\mathbf{B}, c^*)]$ (see text). Oscillations belonging to the H and L series are, respectively, marked by small and long arrows on the $(\mathbf{B}, c^*) = 0^\circ$ curve.

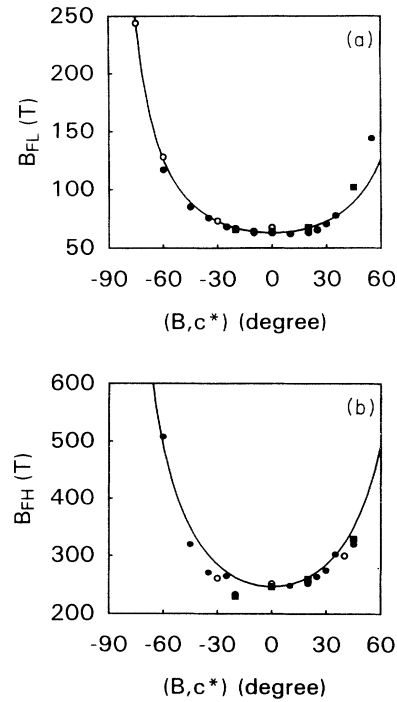


FIG. 9. Tilt angle (\mathbf{B}, c^*) dependence of (a) L and (b) H series oscillation frequencies deduced from data in Fig. 8 (solid circles), sample 1 (open circles), and sample 3 (squares), respectively. Solid lines are fits to a cosine law with $B_{FL}(0) = 63$ T and $B_{FH}(0) = 247$ T, respectively.

law, which is a signature of a 2D behavior, is in good agreement with the data for the L series, only for $(\mathbf{B}, c^*) < +40^\circ$, while an approximate agreement is only achieved for the H series in the whole (\mathbf{B}, c^*) range covered by the experiments. In addition, the phase factor γ is strongly angle dependent. The shift of the oscillations evidenced in Fig. 8 can thus be ascribed to both a deviation from the 2D behavior of $B_{FL(H)}$ and to a tilt angle dependence of the phase factor. Biskup *et al.*²⁹ also report on MR anisotropy measured at 4.2 K in the field range up to 12 T. Their data yield a tilt angle dependence of B_{FL} in good agreement with ours, although they do not mention any shift of the phase factor as the tilt angle varies.

The most striking feature of the data in Fig. 8 is the lack of symmetry, as the tilt angle departs from 0° , between positive and negative (\mathbf{B}, c^*) values, respectively. For example, the H -series oscillations appear at much lower magnetic field in the data at $(\mathbf{B}, c^*) = +20^\circ$ (~ 16 T) than in the data at -20° (~ 20 T). This behavior can be accounted for by the tilt angle dependence of the amplitude of the oscillations. Indeed, as can be seen in Fig. 10, the amplitude of the L series is maximum at $(\mathbf{B}, c^*) \sim -20^\circ$, while the amplitude of the H series exhibits two maxima at about $\pm 20^\circ$. A possible explanation of this peculiar oscillating behavior of the MR could involve some recent calculations of Yakovenko.⁴¹ Indeed, they show that, in the low-temperature metallic state of quasi-1D compounds, the second-order correction to the

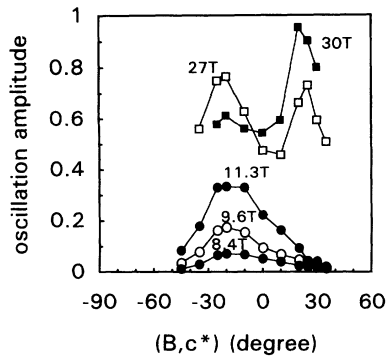


FIG. 10. Tilt angle dependence of the amplitude of some oscillations. Squares and circles, respectively, stand for the H and L series. The corresponding value of B_n (for $\mathbf{B} \parallel c^*$) is indicated on each curve.

free energy due to electron correlations nicely accounts for the oscillations of the magnetization either as \mathbf{B} (Ref. 14) or as the tilt angle⁴² varies in the ClO_4 salt. In both cases, the magnetization oscillations could be linked to MR oscillations.^{14,42} The consequence is that both FO's and CR could have the same physical origin. It is worth noting that the energy scale involved in the calculations is larger than t'_b , and thus they may still work in the SDW phase.⁴¹ We have, however, to be prudent with such an interpretation to account for the deviation from the 2D behavior in the present case of the NO_3 salt. Indeed, (i) no evidence of magic angle features has been reported in the angular dependence of the low-field MR (Refs. 26 and 27) and (ii) neither the maxima nor the minima which appear in Fig. 10 coincides with any magic angle.

IV. CONCLUSION

We have performed transverse magnetoresistance measurements up to 37 T in the organic conductor $(\text{TMTSF})_2\text{NO}_3$ at ambient pressure in the temperature range 2–77 K.

When a magnetic field is applied parallel to the lowest conduction direction c^* in the metallic state above ~ 12 K, MR data can be accounted for by a power law. In the temperature range where AO takes place, a decrease from ~ 3 to ~ 2 of the power-law exponent is evidenced. Although AO should induce closed orbits, no quantum oscillation is evidenced above 12 K, in agreement with previous data recorded in the high-pressure metallic state at 0.5 K.³ At temperatures close to T_{SDW} , the enhancement of the MR may be correlated to the increases of T_{SDW} and probably of the order parameter. The magnetic field dependence of T_{SDW} is in overall agreement with theoretical predictions for the SDW imperfect nesting case.³⁴

Two MR oscillation series are evidenced in the 2–10 K range. While the high-frequency series [$\mathbf{B}_{\text{FH}} = (248 \pm 5)$ T] can be identified as FO's usually observed in Bechgaard salts the low-frequency one, with $\mathbf{B}_{\text{FL}} = (63 \pm 2)$ T, is not linked to any cascade of FISDW transitions. None of these oscillation series can be accounted for by the SdH model, although the low-frequency series could be due to residual carrier pockets.

The angular behavior of these oscillations has been studied at 4.2 K. A deviation from 2D behavior is evidenced, mainly due to a tilt angle dependence (\mathbf{B}, c^*) of the phase factor. Moreover, MR oscillation data are not the same as (\mathbf{B}, c^*) departs from 0° , for positive and negative values, respectively. This is mainly due to the non-monotonous tilt angle dependence of the amplitude of the oscillations. A tentative interpretation is proposed on the basis of Yakovenko's calculations.⁴¹

Finally, both the MR (at $T < 3$ K) and oscillation amplitude of the two series (at $T < 4$ K) decrease as the temperature decreases. This could be understood by assuming that a glass transition takes place in this temperature range.

ACKNOWLEDGMENTS

We are grateful to D. Jerome, G. Montambaux, S. Tomic, and V. Yakovenko for fruitful discussions.

¹D. Jerome, A. Mazaud, M. Ribault, and K. Bechgaard, *J. Phys. Lett. (France)* **41**, L-95 (1980).
²K. Bechgaard, K. Carneiro, M. Olsen, F. B. Rasmussen, and C. S. Jacobsen, *Phys. Rev. Lett.* **46**, 852 (1981).
³W. Kang, S. T. Hannahs, L. Y. Chiang, R. Upasani, and P. M. Chaikin, *Phys. Rev. Lett.* **65**, 2812 (1990).
⁴S. Tomic, J. R. Cooper, D. Jerome, and K. Bechgaard, *Phys. Rev. Lett.* **62**, 462 (1989).
⁵K. Bechgaard, C. S. Jacobsen, K. Mortensen, H. J. Pedersen, and N. Thorup, *Solid State Commun.* **33**, 1119 (1980).
⁶K. Mortensen, Y. Tomkiewicz, T. D. Schultz, and E. M. Engler, *Phys. Rev. Lett.* **46**, 1234 (1981).
⁷P. Garoche, R. Brusetti, and K. Bechgaard, *Phys. Rev. Lett.* **49**, 1346 (1982).

⁸S. Tomic, D. Jerome, P. Monod, and K. Bechgaard, *J. Phys. Lett. (France)* **43**, L-839 (1982).
⁹J. P. Pouget, R. Moret, and R. Comes, *J. Phys. Lett. (France)* **42**, L-543 (1981).
¹⁰J. F. Kwak, J. E. Shirber, R. L. Greene, and E. M. Engler, *Phys. Rev. Lett.* **46**, 1296 (1981).
¹¹K. Kajimura, H. Tokumoto, M. Tokumoto, K. Murata, T. Ukachi, H. Anzai, T. Ishiguro, and G. Saito, *J. Phys. (Paris) Colloq.* **44**, C3-1059 (1983).
¹²M. Ribault, D. Jerome, J. Tuchendler, C. Weyl, and K. Bechgaard, *J. Phys. Lett. (France)* **44**, L-953 (1983).
¹³M. J. Naughton, R. V. Chamberlin, X. Yan, P. M. Chaikin, S. Y. Hsu, L. Y. Chiang, and M. Ya Azbel, *Phys. Rev. Lett.* **61**, 621 (1988).

- ¹⁴X. Yan, M. J. Naughton, R. V. Chamberlin, S. Y. Hsu, L. Y. Chiang, J. S. Brooks, and P. M. Chaikin, *Phys. Rev. B* **36**, 1799 (1987).
- ¹⁵M. Ribault, J. Cooper, D. Jerome, D. Maily, A. Moradpour, and K. Bechgaard, *J. Phys. Lett. (France)* **45**, L-935 (1984).
- ¹⁶J. R. Cooper, W. Kang, P. Auban, G. Montambaux, D. Jerome, and K. Bechgaard, *Phys. Rev. Lett.* **63**, 1984 (1989).
- ¹⁷W. Kang, J. R. Cooper, and D. Jerome, *Phys. Rev. B* **43**, 11 467 (1991).
- ¹⁸A. G. Lebed, *Pis'ma Zh. Eksp. Teor. Fiz.* **43**, 137 (1986) [*JETP Lett.* **43**, 174 (1986)]; A. G. Lebed and P. Bak, *Phys. Rev. Lett.* **63**, 1315 (1989).
- ¹⁹M. Heritier, G. Montambaux, and P. Lederer, *J. Phys. Lett. (France)* **46**, L-831 (1985); G. Montambaux, M. Heritier, and P. Lederer, *Phys. Rev. Lett.* **55**, 2078 (1985).
- ²⁰J. P. Ulmet, A. Khmou, P. Auban, and L. Bachere, *Solid State Commun.* **58**, 753 (1986).
- ²¹J. P. Ulmet, P. Auban, A. Khmou, and S. Askenazy, *J. Phys. Lett. (France)* **46**, L-535 (1985).
- ²²H. Schwenk, S. S. P. Parkin, R. Schumaker, R. L. Greene, and D. Schweitzer, *Phys. Rev. Lett.* **56**, 667 (1986).
- ²³S. Tomic, J. R. Cooper, W. Kang, D. Jerome, and K. Maki, *J. Phys. (France)* **I 1**, 1603 (1991).
- ²⁴A. Mazaud, Ph.D. thesis, University of Orsay, 1981.
- ²⁵V. M. Yakovenko, *Zh. Eksp. Teor. Fiz.* **93**, 627 (1987) [*Sov. Phys. JETP* **66**, 355 (1987)].
- ²⁶M. Basletic, N. Biskup, B. Korin-Hamzic, S. Tomic, A. Hamzic, K. Bechgaard, and J. M. Fabre, *Europhys. Lett.* **22**, 279 (1993).
- ²⁷M. Basletic, N. Biskup, S. Tomic, B. Korin-Hamzic, and A. Hamzic, *Synth. Met.* **55-57**, 2593 (1993).
- ²⁸A. Audouard, F. Goze, S. Dubois, J. P. Ulmet, L. Brossard, S. Askenazy, S. Tomic, and J. M. Fabre, *Europhys. Lett.* **25**, 363 (1994).
- ²⁹N. Biskup, L. Balicas, S. Tomic, D. Jerome, and J. M. Fabre, preceding paper, *Phys. Rev. B* **50**, 12 721 (1994).
- ³⁰F. Goze, A. Audouard, L. Brossard, V. N. Laukhin, J. P. Ulmet, M. L. Doublet, E. Canadell, J. P. Pouget, V. E. Zavodnik, R. P. Shibaeva, B. Hilti, and C. W. Mayer (unpublished).
- ³¹J. P. Ulmet, P. Auban, and S. Askenazy, *Phys. Lett.* **98A**, 457 (1983).
- ³²M. E. Fisher and J. S. Langer, *Phys. Rev. Lett.* **20**, 665 (1968).
- ³³A. Bjelis and K. Maki, *Phys. Rev. B* **44**, 6799 (1991).
- ³⁴G. Montambeaux, *Phys. Rev. B* **38**, 4788 (1988).
- ³⁵J. F. Kwak, J. E. Schirber, P. M. Chaikin, J. M. Williams, H. Wang, and L. Y. Chiang, *Phys. Rev. Lett.* **56**, 972 (1986).
- ³⁶L. M. Falicov and P. R. Sievert, *Phys. Rev.* **138**, A88 (1965).
- ³⁷E. I. Blount, *Phys. Rev.* **126**, 1636 (1962).
- ³⁸J. P. Ulmet, A. Khmou, and L. Bachere, *Physica B* **143**, 400 (1986).
- ³⁹J. C. Lasjonias, K. Biljakovic, P. Monceau, and K. Bechgaard, *Phys. Rev. Lett.* **72**, 1283 (1994).
- ⁴⁰G. Mihaly, Y. Kim, and G. Grüner, *Phys. Rev. Lett.* **66**, 2806 (1991).
- ⁴¹V. M. Yakovenko, *Phys. Rev. Lett.* **68**, 3607 (1992).
- ⁴²M. J. Naughton, O. H. Chung, M. Chaparala, X. Bu, and P. Coppens, *Phys. Rev. Lett.* **67**, 3712 (1991).